

Formation and growth of iron-zinc intermetallics during annealing treatment of galvanized steel

G.K. MANDAL¹*, M. DUTTA², TIPU KUMAR¹, AVIK MONDAL², M.G. WALUNJ¹, S. K. MISHRA¹, S. K. DAS¹, R. PAIS² and L.C. PATHAK¹

¹ CSIR- National Metallurgical Laboratory, Jamshedpur - 831007, India

² Tata Steel Ltd. Jamshedpur - 831007, India

Abstract : The development of desired microstructure of galvanized sheet requires in-depth understanding of the formation and growth kinetics of various Fe-Zn intermetallic phases in the coating during post-treatment after hot dipping of the strip in liquid zinc alloy bath. Keeping this in view, annealing treatment of as-received commercial galvanized sheets, obtained from low (0.135 wt.% Al) and high (0.2 wt.% Al) aluminium containing zinc bath, is carried out to examine the microstructure of annealed sheet with varying strip annealing duration at a fixed galvannealing temperature. The effect of the bath aluminium concentration on the formation of the inhibition layer and on the formation mechanisms of various Fe-Zn intermetallics during subsequent galvannealing (GA) treatment is investigated. Strip annealing simulation is performed using Gleeble® 3800 thermo-mechanical simulator. A detailed characterization of the annealed specimens is carried out to study the galvannealed microstructure produced with varying annealing parameters for both the galvanized specimens obtained from commercial liquid zinc alloy bath with varying aluminium content. A systematic study of annealing treatment of galvanized sheet is performed to enhance the understanding of the role of reacted aluminium present at the interface of the substrate and coating in controlling the nucleation and growth kinetics of Fe-Zn phases to obtain the optimum galvannealed structure. It is observed that high aluminium galvanized bath hinders the formation of the desired sequence of Fe-Zn intermetallics in the coating during annealing treatment. However, galvannealed coating formed using low Al-containing zinc bath shows the desired sequence of various Fe-Zn intermetallics with favourable galvannealed microstructure mainly consisted of compact delta (δ) phase, particularly after annealing for 20s at 470°C.

Key Words: Galvannealing Simulation, Gleeble, Interface, Microstructure and GDOES

INTRODUCTION

There is a remarkable increase in the use of hot-dip galvannealed (GA) sheet products in recent years, particularly in automobile industries. The extensive use of galvannealed sheet is not only due to its affordability but also due to its excellent properties including good corrosion resistance and superior weldability and paintability over galvanized (GI) sheet [1-3]. The industrial production of galvannealed coating in continuous hot-dip galvanized process line requires stringent control of processing parameters for obtaining high quality coating with favorable formation of desired sequence and amount of various iron-zinc intermetallics in the phase structure [4-10]. The production of galvannealed coating involved dipping of pre-heated steel strip into a liquid zinc alloy bath containing aluminium generally less than a critical value (liquid Zn with ~0.135wt.% Al) to favour the formation of extremely thin and/or discontinuous Fe-Al inhibition layer at the substrate-coating interface [11-13]. As soon as steel strip is taken out of the liquid zinc alloy bath, the coated strip is subjected to inline annealing treatment with a suitable combination of annealing temperature and time. The annealing treatment, immediately after hot dipping of steel strip in liquid zinc alloy bath, will assist the solid-state diffusion of iron from substrate surface towards the coating for the favorable formation of various Fe-Zn intermetallic phases within the coating. Optimum galvannealed coating consists of a desired sequence and amount of a range of Fe-Zn intermetallic phases with maximum delta (δ) layer, a very thin layer (generally less than 1 μm) of brittle gamma and gamma₁ (Γ and Γ_1) intermetallic phases at the substrate-delta (δ) phase interface with negligible presence of zeta (ζ) crystals at the top surface location of the coating [14]. Presence of very few zeta (ζ) crystals at the top surface of the coating is preferable to improve the coating paintability. Another aim of galvannealed coated microstructure is to reduce the formation of brittle gamma and gamma₁

* Corresponding Author, E-mail: gopi@nmlindia.org

(Γ and Γ_1) intermetallic phases at the interface of substrate and coating to improve the resistance to powdering and flaking during forming operation.

Optimum galvannealing treatment strives for better control of the outward movement of iron atoms from substrate surface towards coating, which depends on the dissolution kinetics of aluminium rich interfacial layer as well as nucleation and growth mechanisms of individual Fe-Zn phases^[15]. It is noted that formation and growth kinetics of different Fe-Zn intermetallic phases strongly depends on many factors including substrate chemistry, aluminium concentration in liquid zinc bath as well as time-temperature schedule of galvannealing process^[11-16]. Therefore, it is imperative to develop a comprehensive understanding of the formation and growth mechanisms of various Fe-Zn intermetallics in the coating for better control of process parameters to achieve the desired GA microstructure.

Many investigators have studied the galvannealing treatment of galvanized coating by varying the process parameters such as bath aluminium concentration, annealing time and temperature^[1, 15, 17-20]. One of the main focus areas of most of these studies is to establish a good linkage of overall coating iron content and individual Fe-Zn intermetallic phase layer formation with galvannealing process parameters. Keeping in view the stringent requirement of process parameters to produce the desired complex microstructure of galvannealed coating further study in this direction will definitely assist to improve the understanding on formation and growth mechanisms of Fe-Zn phases.

In view of the above, present investigation is carried out to examine the microstructure of the galvannealed sheet with varying annealing duration at a fixed galvannealing temperature. Annealing experiments are performed on as-received commercial galvanized sheets obtained from low (0.135 wt.% Al) and high (0.2 wt.% Al) aluminium containing commercial zinc bath. One of the main aims of this study is to investigate the effect of the bath aluminium concentration on the formation of inhibition layer and on the formation mechanisms of various Fe-Zn intermetallics during subsequent galvannealing (GA) treatment. A systematic study of annealing treatment of galvanized sheet is performed to enhance the understanding of the role of reacted aluminium present at the interface location of the substrate and coating in controlling the nucleation and growth kinetics of Fe-Zn phases to obtain the optimum galvannealed coated structure.

EXPERIMENTAL

The as-received hot dip galvanized (GI) sheets obtained from Plant A and Plant B were used as a starting material for annealing experiments. The GI sheet obtained from Plant A was produced using iron saturated liquid zinc bath having ~0.135 wt.% aluminium. GI specimen of Plant B was obtained using a standard iron saturated liquid zinc galvanized bath containing ~0.2 wt.% aluminium. Both Plant A and Plant B specimens were obtained by dipping the steel substrate into the iron saturated Zn-Al bath for about 4s at the bath temperature of ~460°C. It is understood that specimen dipped into a liquid zinc bath containing a low concentration of aluminium (~0.135 wt.%) is expected to form discontinuous aluminium rich inhibition layer at the substrate-coating interface, whereas GI specimen obtained from high aluminium containing zinc bath will result in the formation of stable continuous Fe-Al based interfacial layer at the substrate-coating interface. Therefore, one of the main aims of this study is to investigate the effect of the bath aluminium concentration on the formation of inhibition layer and on the formation mechanisms of various Fe-Zn intermetallics during subsequent galvannealing (GA) process. The hot dip coated specimens obtained from Plant A and Plant B are refereed as AR-1 and AR-2, respectively in the subsequent text.

Figure 1 shows the schematic representation of a typical thermal cycle generally used in the plant for producing galvannealed (GA) coating. Immediately after dipping in liquid zinc alloy bath, the excess liquid zinc from the substrate surface is removed by air wiping, placed just above the commercial galvanized bath, to obtain the required coating thickness. Therefore, the temperature of the coated surface will be reduced during air wiping. Immediately after air wiping, an induction furnace is used for rapid heating of the coated strip to galvannealing temperature, which is in the range of 450-550°C. Thereafter, the coated strip is isothermally annealed inside the soaking furnace for desired galvannealing duration before air-cooling to room temperature. Based on the operating

parameters of galvannealing plant, the process window for annealing treatment of as-received GI specimens was adopted to study the development of various Fe-Zn phases within the coating by varying the annealing duration for a particular galvannealing temperature.

Based on the plant operating line speed (80-120 mpm), the average residence time for isothermal annealing treatment of as-dipped coated steel sheet in a GA plant was calculated to be in the range of 10-20s. Specimens for annealing experiments were prepared by sectioning the as-received plant specimen with pieces of dimensions 260 mm long and 50 mm wide. These pieces were used for strip annealing simulation using Gleeble® 3800 thermo-mechanical simulator. Figure 2(a) shows the pictorial view of strip annealing simulation along with the position of sample and thermocouples inside the simulation chamber of Gleeble. The as-received galvanized specimens of AR-1 were heated at a linear heating rate of 10°C/s to the isothermal annealing temperature of 470°C with varying time steps of 10, 15 and 20s to study the development of Fe-Zn intermetallic phases in the coating. Immediately after annealing at 470°C for a specific duration, the specimens were forced air-cooled. The AR-2 GI specimens were heated at a relatively faster heating rate of 50°C/s to higher galvannealing temperature of 500°C with varying isothermal holding duration of 0, 5 and 30s. The relatively faster heating rate and higher isothermal annealing temperature with a shorter holding time of 0s and 5s were chosen mainly to capture the dissolution kinetics of thin stable continuous Al-rich inhibition layer, which is expected to be present at the substrate-coating interface of AR-2 GI specimen. Keeping in the view of slower diffusion kinetics of Fe through the inhibition layer, a relative higher isothermal annealing temperature of 500°C with longer holding duration of 30s is also considered.

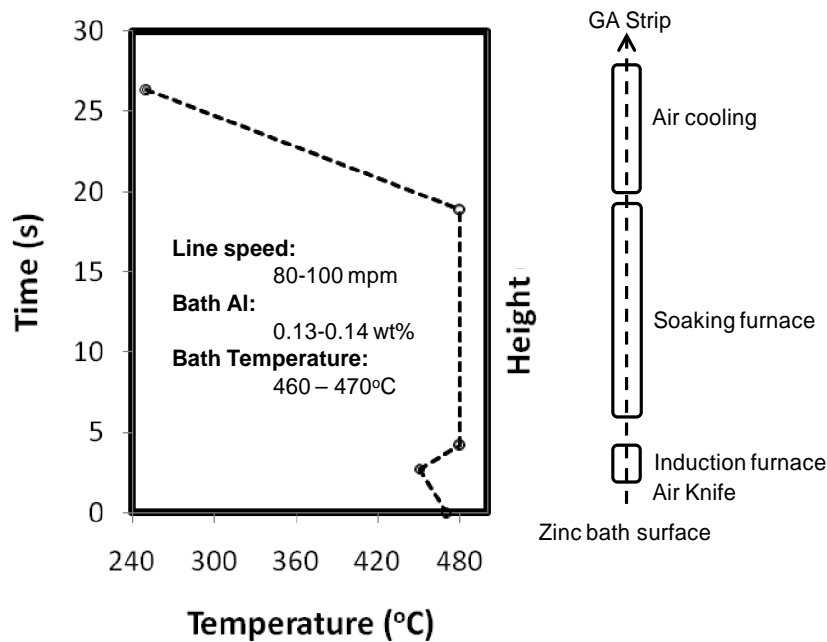


Fig. 1: Schematic representation of a typical galvannealing process

Table 1 summarizes the experimental parameters used for the annealing study. Figure 2(b) shows the picture of a typical galvannealed coating obtained after annealing experiment along with location of three thermocouples attached on the specimen surface. One thermocouple was attached at the centre point on the top surface of the specimen, the second one at 3 cm away from the centre point along the centre line of the specimen in the longitudinal direction and the third one was attached at one side of the strip about 2.5 cm away from the centre point in the width direction. Temperature variations among the thermocouples were within $\pm 2^\circ\text{C}$. Overall temperature variation of the specimen during annealing experiment was within $\pm 5^\circ\text{C}$.

Table 1: Experimental parameters for annealing study

Sample	Heating rate	Annealing temperature (°C)	Annealing time (s)	Cooling condition
AR-1	10°C/s	470	10	Forced Air
			15	
			20	
AR-2	50°C/s	500	0	Forced Air
			05	
			30	

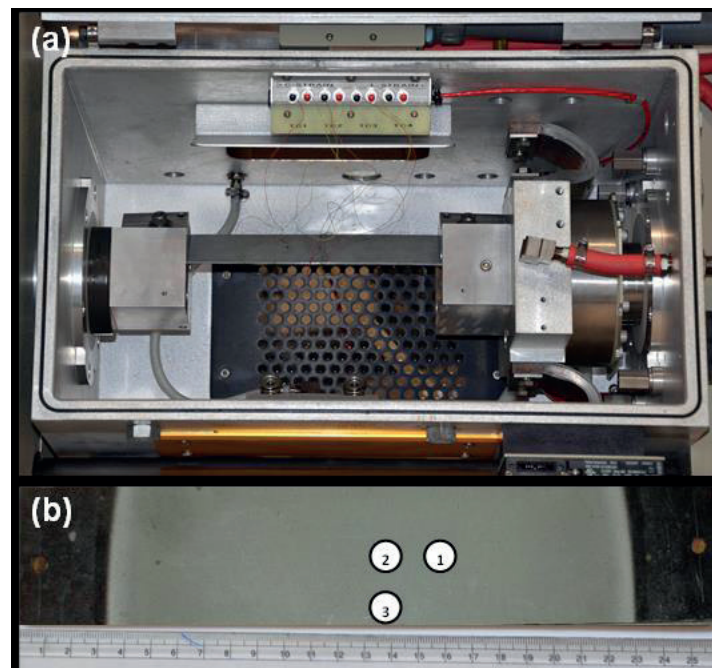


Fig. 2: Pictorial view of (a) strip annealing simulation carried out using Gleeble and (b) specimen after annealing experiment with position of three thermocouples on the specimen surface

The specimens for metallographic characterization were prepared using the standard metallographic techniques. A detailed characterization of the galvanized and galvannealed specimens were carried out using scanning electron microscopy (SEM) attached with Energy-dispersive X-ray spectroscopy (EDS) and glow discharge optical emission spectroscopy (GDOES). GDOES (LECO GDS-850A) was used for the quantitative depth profiling of various elements present in the coating. Quantitative depth profiling plots were taken from top surface of the coating at three different locations from the each specimen. An average of these three GDOES test data obtained from three different locations of the coated surface were used for the estimation of coating thickness and overall coating iron content.

RESULTS AND DISCUSSION

The low magnification cross-sectional scanning electron micrographs of the galvanized coatings (AR-1) reveal the presence of a continuous layer of coating on the substrate surface (Fig. 3). The high magnification SEM images of the plant specimens (AR-1 and AR-2), clearly reveal the coating interface, is given in Fig. 4. The SEM images clearly show the presence of a continuous layer of a coating having a thickness in the range of 5 to 7 μm on the steel substrate for both the coated specimens (AR-1 and AR-2).

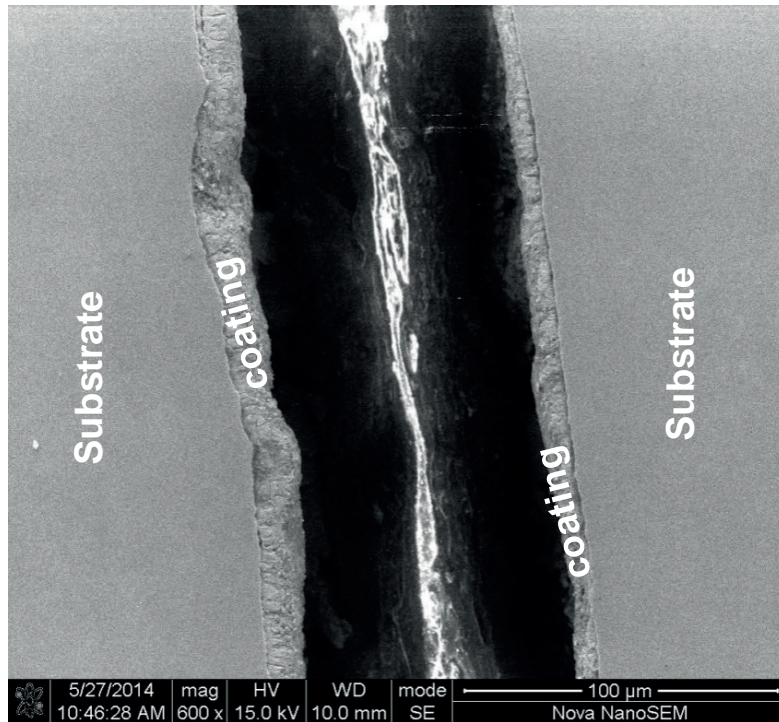


Fig. 3: The cross sectional SEM micrographs of the coatings of the plant specimen

The as-received galvanized coating of AR-1 (Fig. 4(a)) clearly demonstrates the formation of discontinuous Fe-Zn intermetallics of zeta (ζ) crystals with familiar blocky morphology at the interface between substrate and coating. The overlay coating consists of eta (η) phase of mainly pure zinc having a thickness in the range of 4-5 μm , whereas the thickness of zeta (ζ) phase at the substrate-coating interface is in the range of 1-2 μm . It is noted that the presence of zeta (ζ) crystals is completely absent at the substrate-coating interface for the coated specimen of AR-2 (Fig. 4(b)). The AR-2 GI specimen mainly consists of eta (η) layer with a very thin continuous aluminum rich interfacial layer at the interface between substrate and coating. This well-developed Al-rich interfacial layer, which is formed immediately as strip enters into the bath, completely inhibits the formation of zeta (ζ) crystals of iron-zinc intermetallics by preventing the direct contact of solid iron and liquid zinc in the bath. Figure 5 shows the SEM images obtained from the top surface of the coating for both AR-1 and AR-2 specimens. The scanning electron micrographs obtained from the top surface of the coatings clearly demonstrate the presence of only η phase (pure Zn) in both the specimens.



Fig. 4: The cross-sectional SEM micrographs of the coatings of the AR-1 (a) and AR-2 (b) specimens

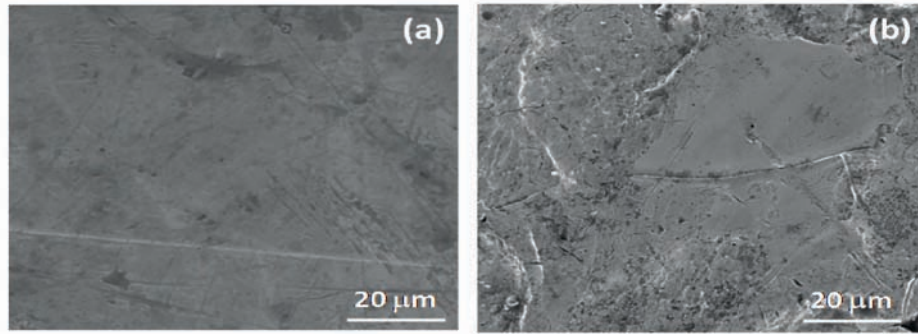


Fig. 5: Top surface of the coating for both these steels (AR-1 and AR-2) reveal the presence of only η phase (pure Zn)

An EDS analyses, conducted for elements aluminum, iron and zinc, of both the as-received specimens (AR-1 and AR-2) across the coating reveal a high intensity peak of aluminum at the interface between substrate and coating, which confirms the formation of an aluminum rich inhibition layer. The overlay coating layer is removed using an acid solution without affecting the Fe-Al based inhibition layer formed at the coating-substrate interface to examine the top surface microstructure of the Al rich layer, for both the as-received specimens. Figure 6 shows the EDS elemental mapping of Zn, Fe and Al, respectively obtained from the top surface of interfacial layer for AR-1 specimen as shown in Fig. 6(a). Elemental distribution maps demonstrate the uniform distribution of aluminium and iron throughout the inhibition layer (Fig. 6(c) & (d)). Elemental distribution map shown in Fig. 6(b) also reveals the segregation of zinc at one location on the surface, as zinc layer is not fully removed from that location of the interfacial layer by acid reaction.

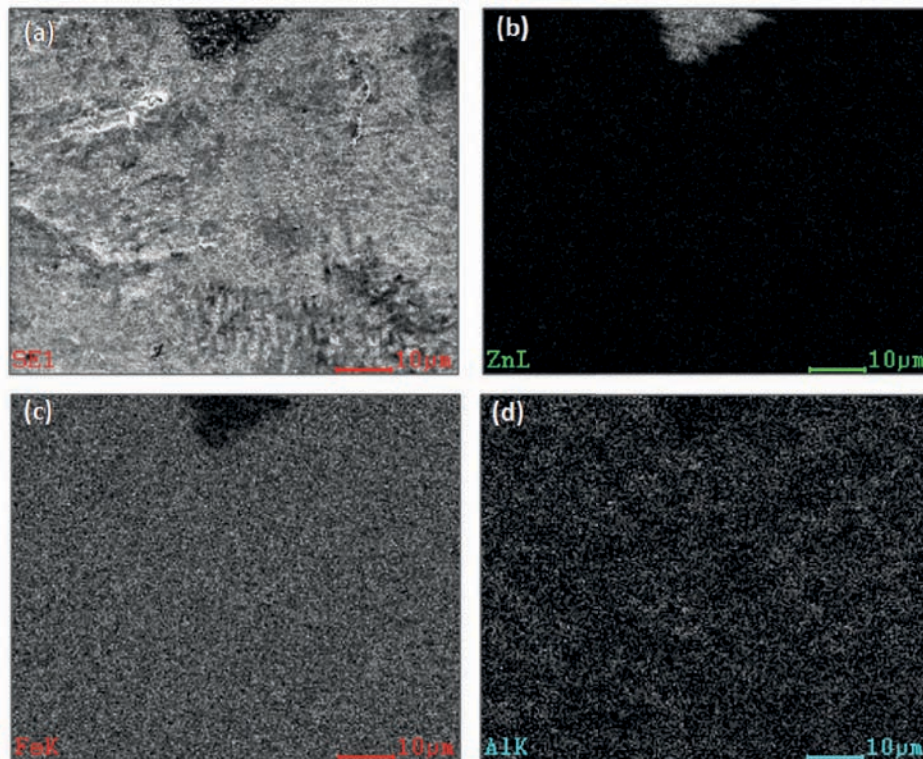


Fig. 6: X-ray mapping of the interfacial layer for the coating: (a) SEM micrograph shows the morphology of the interfacial layer, and (b)-(d) show the X-ray mapping of Zn, Fe and Al, respectively, from the region shown in (a).

The top surface morphology of the Fe-Al interfacial layer, at high magnification, for both the as-received specimens is shown in Fig. 7. It is observed that the aluminum-rich interfacial layer is not compact and continuous

for AR-1 specimen, whereas Fe-Al crystals are densely packed and continuous for AR-2 specimen. The EDS spectra obtained from region of Figs. 7(a) and (c) reveals the strong peaks of Al and Fe. However, intensity of Al peak is weak for AR-1 specimen in comparison to AR-2 specimen. The EDS analysis, therefore, indicates that the presence of higher concentration of Al at the interface for AR-2 specimen. From this analysis, it can be stated that an aluminum rich inhibition layer is formed on the substrate surface at the coating interface and this interfacial layer is expected to be compact and continuous for AR-2 specimen. For AR-1 specimen, this interfacial layer is porous and discontinuous, which will promote the formation of discontinuous zeta (ζ) crystals of Fe-Zn intermetallics at the substrate-coating interface.

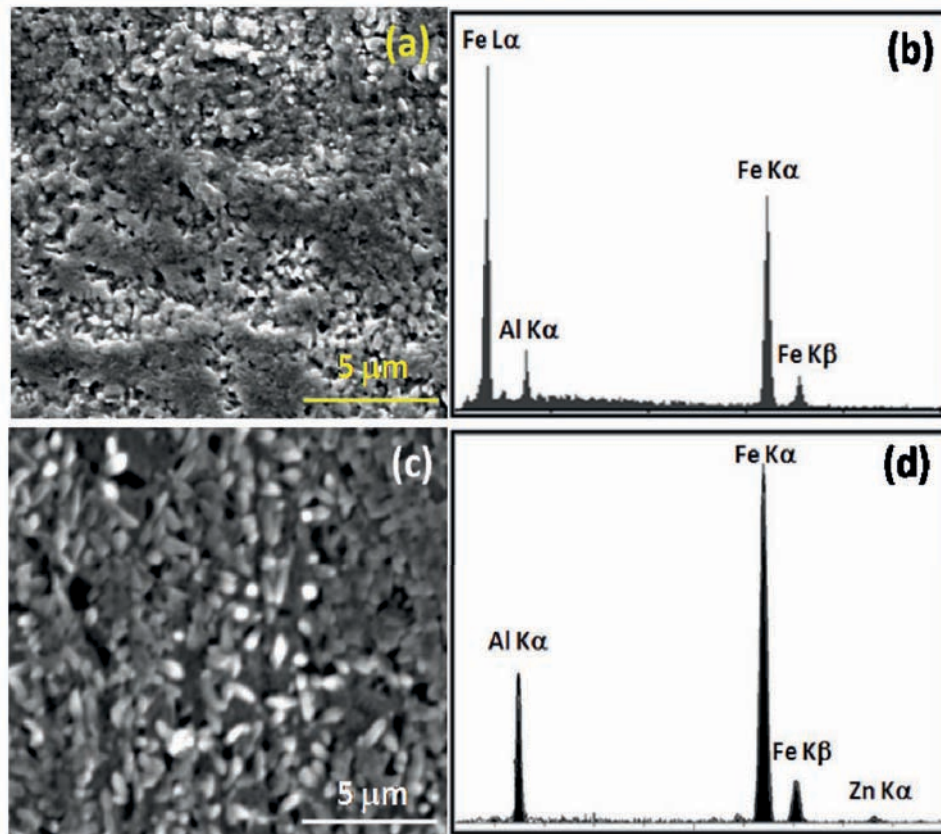


Fig. 7: SEM micrographs (a & c) and EDS analysis (b & d) obtained from top surface of the interfacial layer (a-b: Specimen AR-1; c-d: Specimen AR-2)

The presence of reacted aluminium at the coating interface is further confirmed by analysing the GDOES depth profile data obtained from top surface of both the as-received galvanized specimens. GDOES depth profile data of individual elements for the as-received GI specimens (AR-1 and AR-2) obtained from one of the location of the top surface of the coating is shown in Fig. 8. Elemental profiles indicate that peak position of Al is obtained at coating thickness of about 7.0 and 7.5 μm for AR-1 and AR-2 specimens, respectively. It is also observed that elemental profiles intersect at 50 wt.% for the elements iron and zinc, which is very close to the peak positions of Al for respective samples. Therefore, peak position of aluminium may be considered as substrate-coating interface in case of GI specimens and estimated thicknesses based on the position of Al peak may be considered as approximate thickness of the coatings, which is generally over estimated as iron concentration at this location of the coating is always on much higher side. The GDOES analysis also confirms that Al concentration at the interface location is always higher for the AR-2 specimen than AR-1 specimen. This also indirectly confirms that inhibition layer thickness in AR-2 specimen is more in comparison to AR-1 specimen.

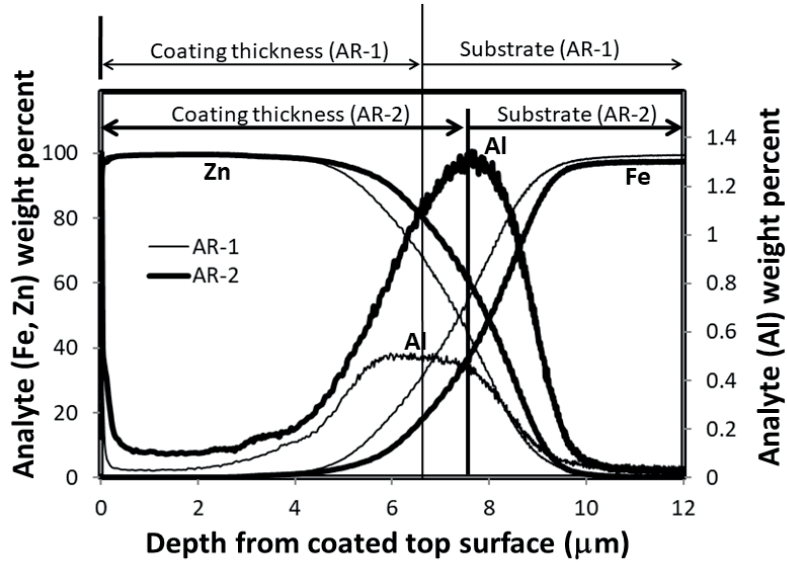


Fig. 8: GDOES plot for as-received GI specimens (AR-1 and AR-2)

Table 2 shows the details of various phases expected in Fe-Zn binary systems particularly for the GI and GA specimens including phase stoichiometry, iron content and density of individual phases [8, 21-23]. The average iron content of various individual phases and phase mixture, as mentioned in the table, is estimated based on the range of iron content in various Fe-Zn intermetallics [8, 23]. The density of individual phases and mixture of two phases is estimated by applying the inverse rule of mixture [8].

Table 2

Various phases expected in Fe-Zn binary systems particularly for the GI and GA specimens along with phase stoichiometry, iron content and density of individual phases [8, 21-23]

Phases	Stoichiometry	Wt% Fe	Average wt% Fe	Density (gm/cc)
α -Fe	Fe	100	100	7.86
η -Zn	Zn	0	0	7.14
$\eta+\zeta$		2.6	7.157
ζ	FeZn_{13}	5.2-6.1	5.65	7.177
$\zeta+\delta$		6.75	7.184
δ	FeZn_{10}	7.4-11.3	9.35	7.202
$\delta+\Gamma_1$		13.75	7.231
Γ_1	$\text{Fe}_5\text{Zn}_{21}$	16.2-18.2	17.2	7.254
$\Gamma_1+\Gamma$		19.25	7.268
Γ	$\text{Fe}_3\text{Zn}_{10}$	20.3-27	23.65	7.298

The elemental profiles, as obtained from GDOES data, are considered to estimate the overall iron and aluminium content of the coatings [8, 23]. The overall iron content of the coating can be estimated as follows:

$$[\text{wt.\% Fe}]_{\text{coating}} = 100 \times \frac{\sum M_{\varphi}^{\text{Fe}}}{\sum M_{\varphi}} \quad (1)$$

where, M_{φ} is the mass of phase layer φ (in Kg) and M_{φ}^{Fe} is the mass of Fe in phase layer φ (kg). These values are estimated as follows:

$$M_{\varphi} = V_{\varphi} \times \rho_{\varphi} \quad (2)$$

$$M_{\varphi}^{\text{Fe}} = V_{\varphi} \times \rho_{\varphi} \times f_{\varphi} \quad (3)$$

Here, V_{φ} is the volume of the φ layer and it is estimated as

$$V_{\varphi} = t_{\varphi} \times L_T \times w_T \quad (4)$$

where, f_{φ} and ρ_{φ} are average weight fraction iron and density (kg.m^{-3}) of a single phase layer or layer consists of mixture of two phases, as indicated in last two column of Table 2. L_T and w_T are overall length and width of coating (in m). t_{φ} is the layer thickness of a Fe-Zn intermetallic phase layer or a layer consisted of mixture of two Fe-Zn intermetallic phases measured from depth profile data of GDOES by superimposing composition range of individual phase layer, as mentioned in the Table 2.

In case of galvanized coating (GI), a correction for overall iron content of the coating is carried out by eliminating the contribution of iron involved in the formation of aluminium rich Fe_2Al_5 layer. It is noted that high affinity of liquid aluminium towards iron results in the formation of iron-aluminide ($\text{Fe}_2\text{Al}_5\text{Zn}_x$) layer on the strip surface during galvanizing process in case of liquid zinc bath containing Al. It is difficult to accurately estimate the iron-aluminide inhibition layer composition as this layer is extremely thin, therefore, in the present study inhibition layer is considered as Fe_2Al_5 [24-25]. By neglecting the Al present in the top surface of the coating, weight percent aluminium in the coating involved for the formation of Fe_2Al_5 layer is estimated from the elemental profile of Al obtained from the GDOES data as follows:

$$[\text{wt.}\% \text{ Al}]_{\text{coating}} = \sum([\text{wt.}\% \text{ Al}] \times d_i) / \sum d_i \quad (5)$$

where, $[\text{wt.}\% \text{ Al}]$ is the average weight percent aluminium within the coating depth d_i . The mass of aluminium (in kg) reacted for the formation of Fe_2Al_5 layer at the coating interface:

$$M_{\text{Fe}_2\text{Al}_5}^{\text{Al}} = ([\text{wt.}\% \text{ Al}]_{\text{coating}} \times \sum M_{\varphi}) / 100 \quad (6)$$

Mass of Fe_2Al_5 layer ($M_{\text{Fe}_2\text{Al}_5}$) and mass of iron involved for the formation of Fe_2Al_5 layer ($M_{\text{Fe}_2\text{Al}_5}^{\text{Fe}}$) are as follows:

$$M_{\text{Fe}_2\text{Al}_5} = 1.82 \times M_{\text{Fe}_2\text{Al}_5}^{\text{Al}} \quad (7)$$

$$M_{\text{Fe}_2\text{Al}_5}^{\text{Fe}} = 0.45 \times M_{\text{Fe}_2\text{Al}_5} \quad (8)$$

The estimated thickness of Fe_2Al_5 layer formed at the interface

$$t_{\text{Fe}_2\text{Al}_5} = M_{\text{Fe}_2\text{Al}_5} / (\rho_{\text{Fe}_2\text{Al}_5} \times L_T \times w_T) \quad (9)$$

Here, $\rho_{\text{Fe}_2\text{Al}_5}$ is the density of Fe_2Al_5 layer, which is considered as 4720 kg/m^3 [25].

The overall Fe content of the GI coating (in wt.%)

$$[\text{wt.}\% \text{ Fe}]_{\text{coating, GI}} = 100 \times (\sum M_{\varphi}^{\text{Fe}} - M_{\text{Fe}_2\text{Al}_5}^{\text{Fe}}) / \sum M_{\varphi} \quad (10)$$

Table 3 shows the estimated values of coating thickness, iron and aluminum contents as well as inhibition layer thickness estimated based on above mentioned methods using the Fe and Al depth profiles obtained by GDOES data. For the estimation of coating thickness, GI coating is considered to be consisted of only a single layer, which is a mixture of η and ζ phases, for AR-2 specimen with iron content at the substrate-coating interface is limited to 5.2 wt.%. For AR-1 specimen, overall coating thickness is estimated by assuming two layered structure of coating consisted of a mixture of overlay ($\eta+\zeta$) layer and single phase ζ layer with coating iron content of maximum 6.1 wt.% at the substrate-coating interface. The inhibition layer thicknesses estimated based on the analysis of

GDOES data are ~43 nm and ~83 nm for AR-1 and AR-2 specimens, respectively. These estimated thicknesses are reasonably good agreement with the literature data [18, 26]. Figure 9 shows that the aluminium content in the coating increases with bath Al content. Aluminum content in the inhibition layer estimated in the present study is compared with the data reported by other researchers [18, 26]. Estimated interfacial aluminium content corroborates well with the reported data of Taniyama et al. [26]. However, measured values of reacted aluminium reported by Kanamaru et al. [18] is slightly on higher side in comparison to the amount of aluminium estimated in the present study for the formation of inhibition layer. These slight differences in values are mainly due to difference in measurement techniques as well as variation in galvanizing process parameters particularly the bath temperature. Many investigators also studied the formation and growth of inhibition layer and highlighted that inhibition layer on the strip surface becomes continuous when the crystal size reaches a critical value, which is generally in the range of 40-50 nm [11, 13, 25]. Therefore, inhibition layer thickness estimated in the present investigation clearly indicates that Al rich interfacial layer formed on the strip surface will be very thin and discontinuous for AR-1 specimen, whereas this interfacial layer will be relatively thick, stable and continuous for AR-2 specimen.

Table 3

Estimated values of coating thickness, coating iron and aluminum contents as well as inhibition layer thickness for as-received GI specimens

Sample	Phase layer/s	Coating thickness (Micron)	Coating Al%	Coating Fe%	Inhibition layer thickness (nm)
AR-1	($\eta+\zeta$) & ζ	5.47	0.26	2.43	43.03
AR-2	($\eta+\zeta$)	5.23	0.58	2.13	82.93

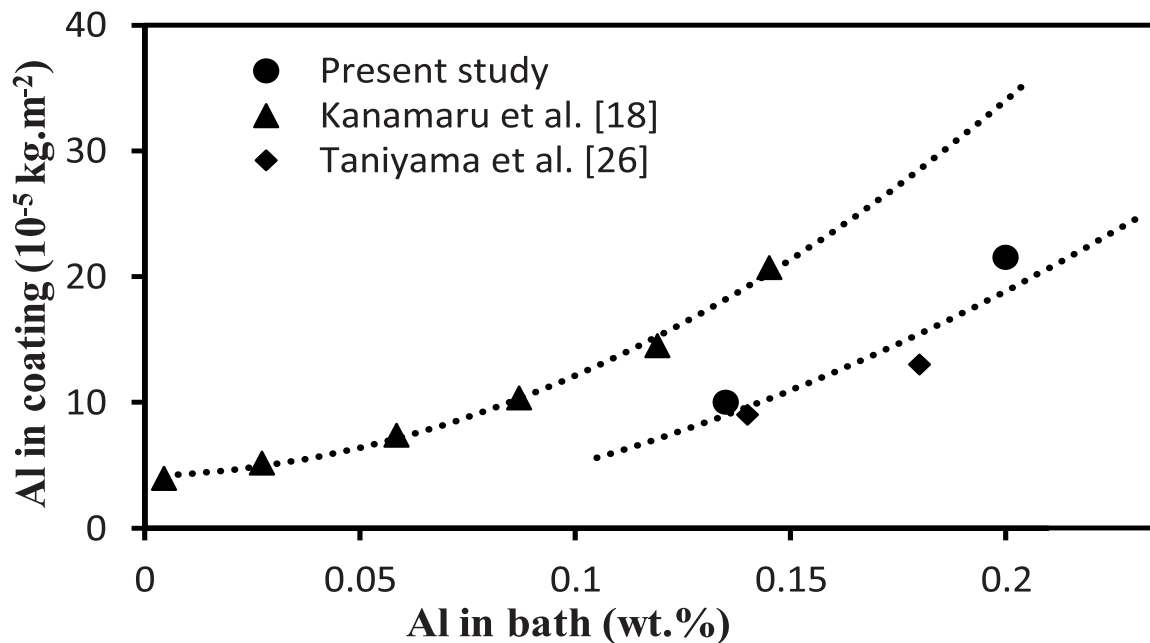


Fig. 9: Variation of Al content in coating with bath Al content

Figure 10 shows the cross-sectional SEM images of the AR-1 specimen isothermally annealed at 470°C with varying galvannealing duration of 10s, 15s and 20s. Micrographs reveal the progress of various Fe - Zn intermetallic layers as a function of annealing duration. Annealing treatment for a short duration of 10s resulted for the development of microstructure mainly consisted of delta (δ), zeta (ζ) and overlay eta (η) phases. However, at the substrate-delta (δ) phase interface a very thin discontinuous layer of gamma phase is clearly visible. Micrographs

also indicate the formation of many voids within the transverse section of the coating (indicated by an arrow in the micrographs). It is also observed that the presence of voids within the coating decreases with increase in annealing duration. It is reported that void formation in the coating occurs when eta (η) phase is consumed by the formation of zeta (ζ) Fe-Zn intermetallic phase because of change in volume due to the appearance of zeta (ζ) crystals^[7]. The decrease in voids formation with the increase in galvannealing times further indicates that coating iron content increases with increase in annealing duration as zeta (ζ) phase layer is consumed by the formation of delta (δ) phase. Specimen isothermally annealed for 15s clearly demonstrates that the coating mainly consists of delta (δ) phase and the presence of (η) phase towards the top surface region of the coating is decreased significantly due to the formation and growth of zeta (ζ) crystals. Specimen isothermally annealed for a longer duration of 20s reveals the growth of compact delta (δ) phase with the decrease in the amount of zeta (ζ) crystals and negligible presence of eta (η) phase at the top surface of the coating. It is also observed the presence of a relatively thick and continuous brittle gamma Fe-Zn intermetallic layer at the interface between substrate and coating. Therefore, it can be stated that AR-1 specimen annealed for 20s results in favourable galvannealed microstructure mainly consisted of compact delta (δ) phase. Presence of many cracks, particularly perpendicular to strip surface, is also observed in all the annealed specimens. However, the formation of cracks and other defects (mainly voids) is minimum for the coated specimen annealed for 20s.

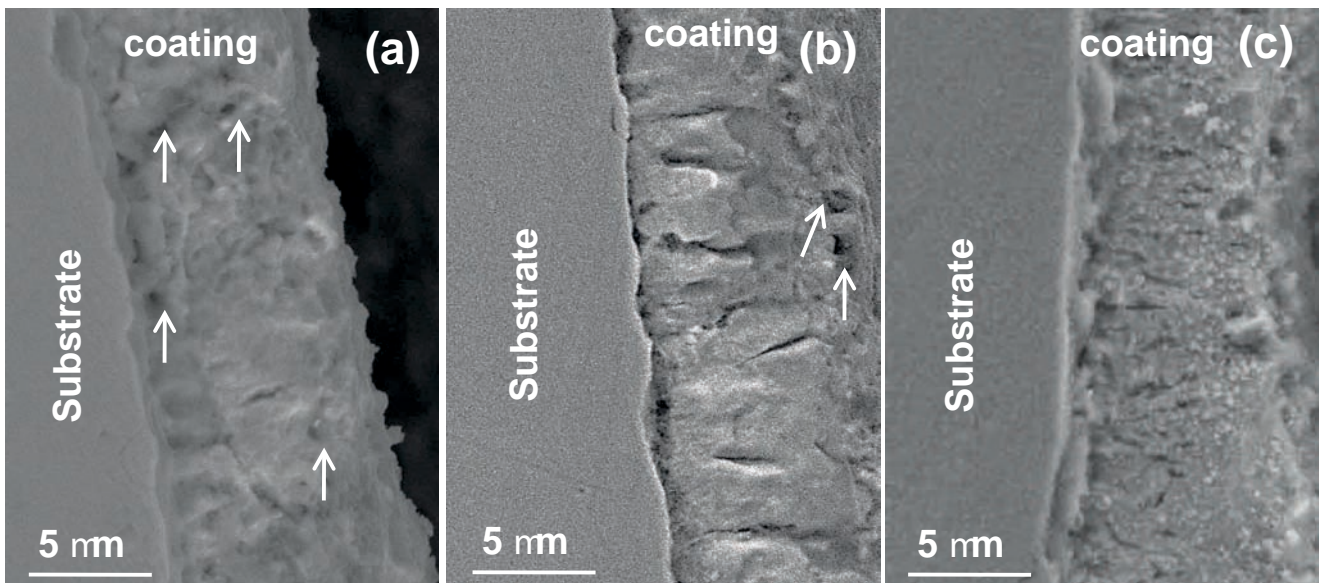


Fig. 10: Cross sectional SEM micrographs of the coating annealing at 4700C with varying galvannealing duration of 10s (a), 15s (b) and 20s (c)

Scanning electron micrographs reveal the top surface morphology of the AR-1 specimen annealed at 470°C for varying durations (Fig. 11). As-received specimen annealed for 10s reveals that the morphology of the top surface of the coating mainly consists of fine blocky zeta (ζ) crystals along with eta (η) phase. However, the amount of eta phase on the coated top surface decreases with the increase in annealing duration. Growth of zeta (ζ) crystals at the expense of eta (η) phase can clearly be seen from the micrographs of the specimen annealed for 15s. The micrograph in Fig. 11(d), at higher magnification, clearly demonstrates that coated top surface mainly consists of a mixture of fine and coarse crystals of zeta (ζ) Fe-Zn intermetallics along with the presence of eta (η) phase at some of the location. Top surface morphology of the specimens annealed for 20s mainly reveals the blocky crystals of zeta phases with the negligible presence of eta (η) phase. Therefore, analysis of top surface confirms that with the increase in annealing time the iron content in coating increases and top surface composition changes from pure zinc to iron-zinc intermetallics.

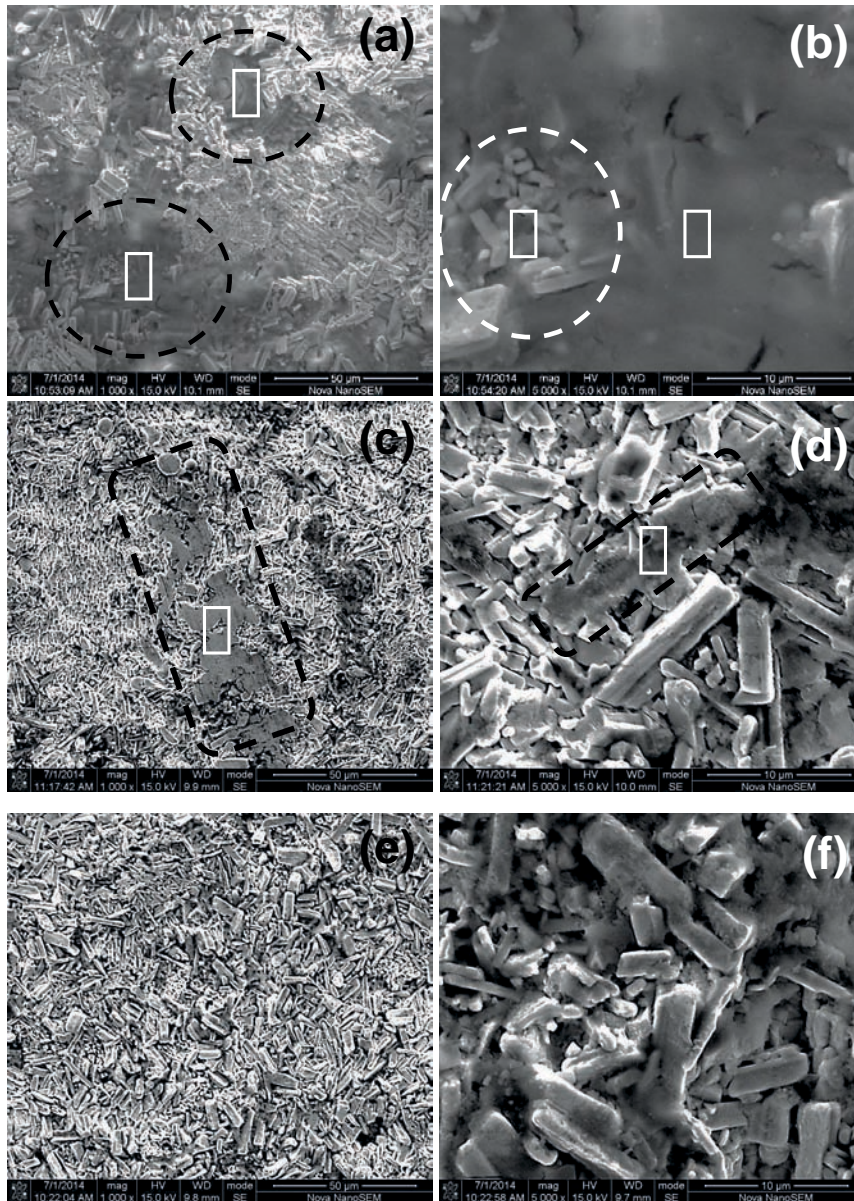


Fig. 11: Scanning electron micrographs revealing the top surface of the coating for the specimens annealed at 470°C for 10s (a & b), (c & d) 15s & (e & f) 20s

Figure 12 shows the cross-sectional SEM micrographs of the AR-2 specimen isothermally annealed at 500°C with varying galvannealing duration of 0s, 5s and 30s. It is noted that this specimen was galvanized using iron saturated liquid Zn-0.2 wt.% Al bath. Therefore, the formation of a continuous Al-rich inhibition layer at the substrate-coating interface is observed for this GI specimen. It is also expected that the presence of this continuous compact inhibition layer will slow down the diffusion assisted formation and growth kinetics of Fe-Zn intermetallic during annealing of the coating. These observations can clearly be explained by analyzing the micrographs of annealed specimens as shown in Fig. 12. Micrographs clearly demonstrate that even after 30s of annealing at a higher annealing temperature of 500°C, the coated microstructure is not fully alloyed coating rather it exhibits mainly the presence of zeta (ζ) crystals. Presence of many voids particularly at the zeta (ζ) crystals location in all the coated specimens clearly indicates that eta (η) phase is consumed by the formation of zeta (ζ) Fe-Zn intermetallic phase. With the increase in annealing time, formation and growth of zeta (ζ) crystals are clearly visible. Specimen after annealing for 30s exhibits the presence of the mainly zeta (ζ) crystals in the

coating with the negligible presence of delta (δ) phase at the substrate-coating interface location. Figure 13 shows the SEM images obtained from the top surface of the AR-2 specimen annealed at 500°C for varying durations of 0s and 30s. The top surface morphology of the annealed specimens reveals the presence of main eta (η) phase. Presence of few zeta (ζ) crystals can also be seen at some of the locations of the top surface. The amount of zeta (ζ) crystals at the top surface is more for the specimen annealed for 30s in comparison to specimen annealed for 0s. The analysis of micrographs of both the annealed specimens (AR-1 and AR-2) clearly demonstrates that formation and growth kinetics of Fe-Zn intermetallics are very slow in AR-2 specimen in comparison to AR-1 specimen. The present study clearly demonstrates that high aluminium (0.2 wt.%) containing zinc bath results in the formation of continuous compact inhibition layer in the GI specimen, which in turn reduced the formation and growth kinetics of Fe-Zn intermetallics during annealing treatment of galvanized coating.

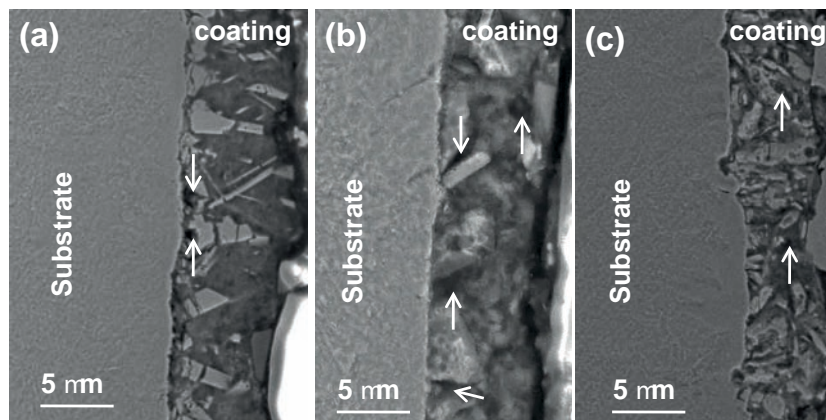


Fig. 12: Cross-sectional SEM micrographs of the coating (AR-2) annealing at 500°C with varying galvannealing duration of 0s (a), 5s (b) and 30s (c)

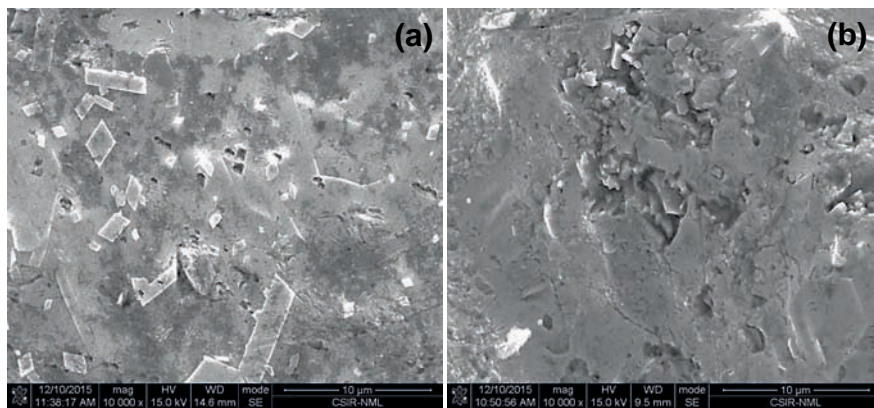


Fig. 13: SEM micrographs reveal the top surface of the coating for the specimens annealed at 500°C for 0s (a) and 30s (b)

In order to further investigate the role of inhibition layer in the formation and growth of various Fe-Zn intermetallics during annealing treatment of galvanized steel, EDS analysis was conducted along the transverse section of the coating for all the annealed specimens of AR-1 and AR-2 sheets. SEM-EDS line scan along the coating cross-section reveals no peak of aluminium at the substrate-coating interface for most of the specimens annealed at 470 and 500°C except the AR-2 specimen annealed for 0s and 5s at 500°C. Figure 14 shows the variation of aluminium concentration along the cross-section of the coating for AR-2 specimen annealed for 0s and 5s at 500°C. EDS line analysis along the transverse section of the coating clearly demonstrates that high concentration of Al at the substrate-coating interface for both the specimens obtained after annealing at 500°C for the duration of 0 and 5s, respectively. It is also noted that no peak of Al at the interface is obtained after about 5s of annealing. Based on the EDS line analysis of Al, it can be stated that thickness of the Al-rich inhibition layer, formed at the substrate-coating interface during the galvanizing process, slowly decreases with annealing duration and eventually disappear after a certain duration of galvannealing.

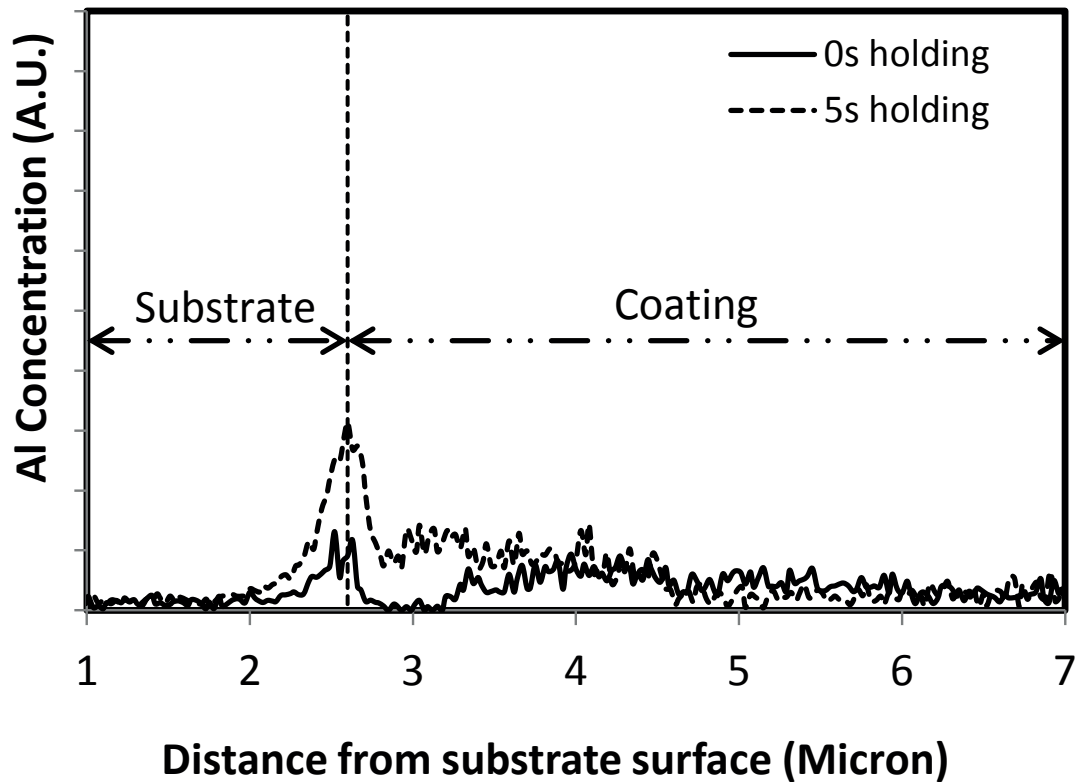


Fig 14: Variation of aluminium concentration along the cross section of the coating for AR-2 specimen annealed for 0s and 5s at 500°C

The EDS analysis across the coating cross-section also indicates higher iron content within the coating for longer annealing duration at a fixed galvannealing temperature. However, a good correlation about the overall coating iron content with galvannealing duration was difficult to obtain based on SEM-EDS analysis. Therefore, GDOES analysis was carried out mainly to find out a suitable correlation between overall iron content of the coating with annealing duration. GDOES analysis was carried out for AR-1 annealed specimens only, as fully alloyed coating was not obtained for the AR-2 annealed specimens. The GDOES plot for one of the annealed specimens obtained from a specific location of top surface is shown in Fig. 15. The layer thickness of a Fe-Zn intermetallic phase layer or a layer consisted of mixture of two Fe-Zn intermetallic phases measured from depth profile data of GDOES by superimposing composition range of individual phase layer^[8]. The average of three values, obtained from three different locations from the top surface of each specimen, is considered for the analysis of overall coating iron content. Table 4 shows the measured average coating thickness of various iron-zinc intermetallic phase layers obtained by analysing the GDOES data. From Table 4, it can be summarized that thickness of delta (δ) and gamma (Γ_1 and Γ) phase layers are comparable for all the three annealed specimens based on the fraction of thickness coverage of overall coating by individual phase regions. However, overall thickness coverage by zeta (ζ) and ($\zeta+\eta$) mixed phase layers decrease for the specimens annealed for longer duration of 15 and 20s. This observation indicates that formation of various Fe-Zn intermetallic phases in the galvannealed coating is controlled by outward diffusion of Fe from strip surface towards the coating. Decrease in zeta (ζ) and ($\zeta+\eta$) phase layer also indicate coating iron content approaches more towards optimal value for the specimen annealed for longer duration of 20s. Therefore, it can be concluded that galvannealing coating with better properties can be obtained for the specimen annealed at 470°C for 20s. This specimen also reveals that brittle gamma ($\Gamma_1+\Gamma$) phase layer thickness is limited to less than 1mm of thickness.

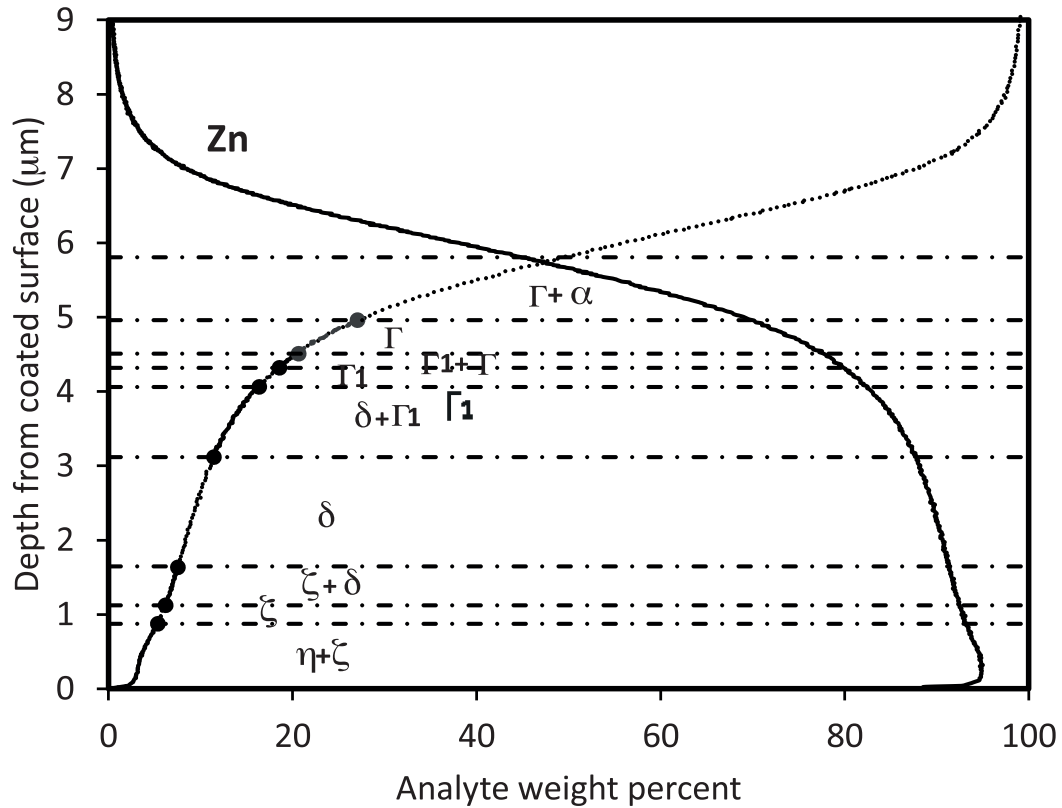


Fig. 15: GDOES plot for the specimen annealed for 10s at 470°C

Table 4: Coating thickness of various phases obtained by GDOES analysis

Phase/s	Annealing duration (s)		
	10	15	20
	Thickness of phase layers (mm)		
η+ζ	1.053	0.882	0.764
ζ	0.308	0.218	0.216
ζ+δ	0.586	0.325	0.39
δ	1.614	1.554	1.383
δ+Γ ₁	0.937	1.367	0.972
Γ ₁	0.252	0.331	0.235
Γ ₁ +Γ	0.208	0.252	0.197
Γ	0.436	0.53	0.466
Overall coating thickness (μm)	5.395	5.459	4.625

Figure 16 shows that variation of average weight percent of iron in the coating with galvannealing time. In the same figure, a model equation (Eq. 11) is also fitted by considering the rate of change of coating iron concentration is directly proportional to the difference between saturated coating iron concentration and instantaneous iron concentration in the coating^[19-20]. The integral form of the equation for the estimation of coating iron content (W_{Fe} , in wt.%) can be written as:

$$W_{Fe} = W_0 + (W_s - W_0) \{1 - \exp(-kt)\} \quad (11)$$

Here, W_0 is the initial iron content in the coating before the start of galvannealing treatment, which is 2.43 wt.% for AR-1 specimen (refer Table 2), W_s is the saturated iron content in the coating (wt.%), t is the galvannealing time (s) and k is model parameter (s^{-1}). The values of W_s and k are estimated as 13 wt.% and $0.105 s^{-1}$, respectively by best fitting the experimental data in the model equation. The estimated values of these model parameters are in good agreement with literature data [19-20]. In Figure 16, experimental data of coating iron content obtained by Santos et al. [20] and Lin et al. [15] are also included. For comparison purpose, the variations of coating iron content with galvannealing time for the specimen annealed at 475°C using Zn-0.1 wt.% Al bath, as reported by Santos et al., is included [20]. Lin et al. studied the galvannealing behaviour at 500°C with varying galvannealing time for two different grades of steel (designated as IF and IFP) using Zn-0.14 wt.% Al bath and observed the variation of coating iron content with galvannealing time. Overall coating iron content predicted based on Eq. 11 corroborates well with the present data estimated based on GDOES analysis as well as experimental data reported in literature for galvannealing duration of 10 s and more. Experimental data of coating iron content reported in literature for shorter galvannealing duration (less than 10s) are on higher side compare to predicted value based on Eq. 11. It should be noted that coating iron content just after dipping in liquid zinc bath is expected to be lower than the value (~ 8 wt.% Fe) reported by them. This is mainly due to application of shorter dipping time and presence of Al (0.1 to 0.14 wt.% Al) in liquid zinc bath during galvanizing process. It is also noted that during annealing treatment of galvanized steel coating iron content and formation of various Fe-Zn intermetallics in the coating is mainly controlled by solid state diffusion of iron from substrate towards the coating. Therefore, kinetics of solid state iron diffusion through various Fe-Zn intermetallic phases in the coating is expected to be sluggish.

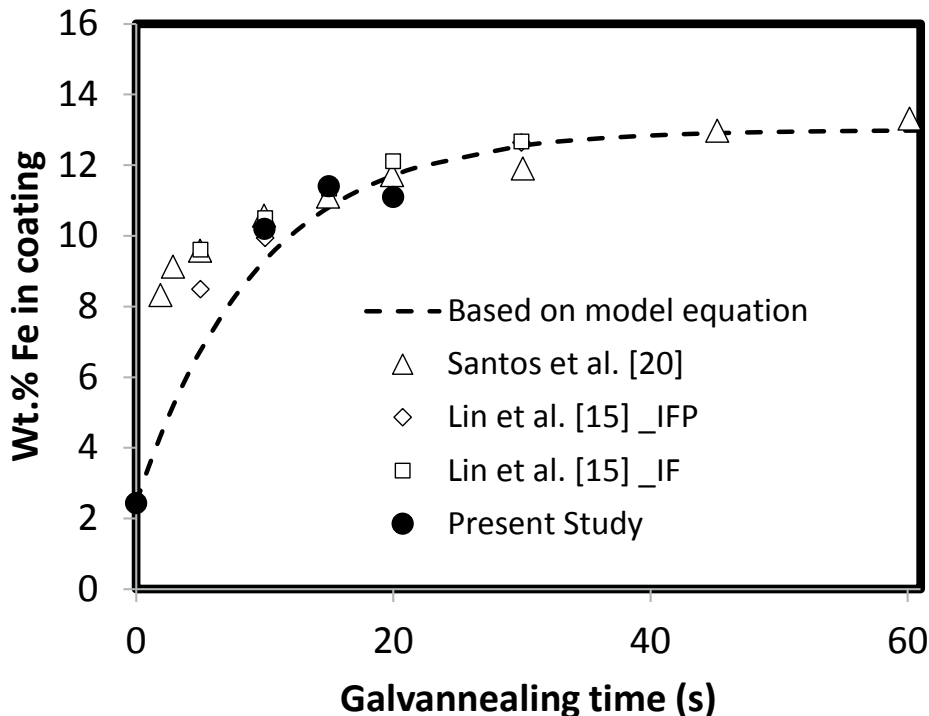


Fig. 16: Variation of average weight percent of iron in coating with galvannealing time

In the present study, galvannealing treatment of galvanized steels, obtained using low (0.135 wt.% Al) and high (0.2wt.% Al) Al containing commercial liquid zinc bath, is carried out to study the formation and growth mechanisms of various Fe-Zn intermetallics in the coating. It is observed that low Al containing Zn bath results in the formation of thin and discontinuous inhibition layer at the interface between substrate and coating of GI sheet. This inhibition layer was insufficient to prevent the direct contact between liquid zinc and solid iron. Therefore, GI sheet obtained using low Al zinc bath shows the formation of discontinuous

Fe-Zn intermetallic zeta (ζ) crystals at the interface location between substrate and coating. It is also observed that GI specimen produced using high Al zinc bath comprises of stable continuous inhibition layer at the substrate-coating interface, which completely inhibits the formation of Fe-Zn intermetallics in the coating. Present study also highlighted that formation and growth kinetics of various Fe-Zn intermetallics are relatively faster in GI specimen produced using low Al zinc bath in comparison to high Al zinc bath. Therefore, galvanized coating formed using low Al containing GI specimen shows the desired sequence and amount of various Fe-Zn intermetallics, particularly after annealing for 20s at 470°C. The sluggish kinetics of formation and growth of Fe-Zn intermetallics during galvannealing treatment of high Al containing galvanized steel is mainly due to the presence of continuous inhibition layer on the substrate surface. It is well understood that the formation and growth of different Fe-Zn phases during galvannealing treatment is primary controlled by diffusion of iron from the substrate surface towards the coating^[16, 27]. Therefore, initial formation and growth of Fe-Zn phases in the Zn coating are controlled by solid-state diffusion of iron through inhibition layer during subsequent annealing treatment just after galvanizing in liquid Zn alloy bath. The kinetics data of diffusion coefficient of Fe (m^2/s) in various phases are calculated based on the Arrhenius correlation [Eq. 12] using the values of pre-exponential constant (D_0) and activation energy (Q) obtained from available literature^[16, 25, 28-30].

$$D = D_0 \exp[-Q/RT] \quad (12)$$

where R is the gas constant (8.314 J/mol.K)

Table 5 shows the kinetics data of diffusivity of iron including D_0 and Q values obtained from the literature^[16, 22, 28-30]. In order to get an idea about the diffusivity data of iron through the inhibition layer, iron diffusion in Al matrix is considered^[25]. From the table, it is clear that there is a significant variation of diffusion of iron through different intermetallic phases. It is also noted that mobility of iron through inhibition layer will be extremely sluggish in comparison to the mobility of Fe through various Fe-Zn intermetallics, particularly in Zeta (ζ) and Delta (δ) phases. Therefore, thick, compact and continuous Al-rich inhibition layer on the substrate surface of GI coating, produced in high Al (0.2 wt.% Al) containing zinc bath, is not suitable to obtain the desired sequence and amount of various Fe-Zn intermetallics in GA coating. Fe diffusivity data clearly suggests that the stable inhibition layer will drastically reduce the formation and growth kinetics of these Fe-Zn intermetallics in the coating. On the other hand extremely thin and/or discontinuous inhibition layer formed during the galvanizing process using low aluminium (0.135 wt.% Al) zinc bath is suitable to obtain desired iron-zinc intermetallic phases in galvanized coating using optimized annealing parameters. The present investigation also reveals that inhibition layer thickness decreases and eventually disappears with the progress of galvannealing time. Therefore, presence of extremely thin and/or discontinuous inhibition layer at the substrate-coating interface will provide better control of Fe diffusivity during the initial period of galvannealing process for the formation of desired amount and sequence of Fe-Zn intermetallics. It is also observed that overall iron content in the coating increases with increase in galvannealing time. From Fig. 16, it can be stated that overall Fe content in the coating increases with increasing rate during the initial period of galvannealing. This is mainly due to the availability of higher driving force for the Fe flux towards coating from the substrate surface due to the low concentration of Fe in the coating during the initial period of galvannealing. The increasing rate of overall iron content in the coating during initial stages of galvannealing process is also due to faster dissolution of extremely thin and discontinuous inhibition layer. Figure 16 also demonstrates that with further increase in galvannealing time overall Fe content in the coating increases at a decreasing rate. This may be due to the formation and growth of Gamma1 (Γ_1) and Gamma (Γ) layers with the progress of the galvannealing process. From Table 5, it can be stated that presence of Gamma1 (Γ_1) and Gamma (Γ) layers at the interface location of substrate and coating is expected to reduce the mobility of Fe and therefore, reduce the rate of increase of overall iron content in the coating with the progress of galvannealing duration.

Table 5 : Kinetics data of diffusivity of iron including D_0 and Q values obtained from literature [16, 25, 28-30]

Phase	Q (kJ/mol)	D_0 (m ² /s)	D (m ² /s)
Zeta (ζ) [16, 28]	99.6	$1.0 \cdot 10^{-4}$	$9.947 \cdot 10^{-12}$
Delta (δ) [16, 28]	106.8	$1.03 \cdot 10^{-4}$	$3.19 \cdot 10^{-12}$
Gamma ₁ (Γ_1) [14, 29]	80	$2.04 \cdot 10^{-8}$	$4.84 \cdot 10^{-14}$
Gamma (Γ) [14, 29]	85.35	$5.0 \cdot 10^{-9}$	$4.994 \cdot 10^{-15}$
Aluminium [20, 30] (Fe ₂ Al ₅ layer)	31.84	$1.7 \cdot 10^{-12}$	$9.82 \cdot 10^{-15}$

SUMMARY AND CONCLUSIONS

In the present investigation, the galvanized strip, obtained from low (0.135 wt.% Al) and high (0.2wt.% Al) Al containing commercial liquid zinc bath was annealed at a fixed galvannealing temperature with varying duration to examine the evolution of the microstructure of galvanized steel during strip annealing simulation. Strip annealing simulation was performed using Gleeble 3800 simulator. The main findings of the present investigation are as follows:

- ✓ Iron saturated galvanizing bath having 0.135 wt.% Al results in the formation of thin and discontinuous inhibition layer at the interface between substrate and coating of GI sheet
- ✓ GI sheet obtained using low Al (0.135 wt.% Al) zinc bath shows the formation of discontinuous Fe-Zn intermetallic zeta (ζ) layer at the interface location between substrate and coating
- ✓ GI specimen produced using high Al (0.20 wt.% Al) zinc bath comprises of stable continuous inhibition layer at the substrate-coating interface, which completely inhibits the formation of Fe-Zn intermetallics in the coating
- ✓ The formation and growth kinetics of various Fe-Zn intermetallics are sluggish in nature in GI specimen produced using high Al zinc bath in comparison to low Al zinc bath
- ✓ Galvannealed coating formed in low Al containing zinc bath shows the desired sequence of various Fe-Zn intermetallics with favorable microstructure suitable for producing GA coating, particularly after annealing for 20s at 470°C
- ✓ The sluggish kinetics of Fe-Zn intermetallics formation during galvannealing treatment of high Al containing galvanized steel is mainly due to the presence of thick and continuous inhibition layer on the substrate surface
- ✓ During galvannealing, inhibition layer thickness decreases and eventually disappears with the progress of galvannealing time
- ✓ Presence of extremely thin and/or discontinuous inhibition layer at the substrate-coating interface will provide a better control of Fe diffusivity during the initial period of galvannealing process for the formation of desired amount and sequence of Fe-Zn intermetallics
- ✓ It is noted that over all Fe content in the coating increases rapidly during initial period of galvannealing. However, with progress of galvannealing time, overall Fe content in the coating increases at a decreasing rate

REFERENCES

- [1] C.S. Lin, M. Meshii and C.C. Cheng: ISIJ Int., 35: 491,1995
- [2] F.M. Queiroz and I. Costa: Surf. Coat. Tech., 201: 7024, 2007
- [3] H.Y.Ha, S.J. Park, J.Y. Kang, H.D.Kim and M.B.Moon: Corros. Sci., 53 : 2430J, 2011
- [4] Inagaki, M. Sakurai and T. Watanabe: ISIJ Int., 35: 1388, 1995
- [5] Z.W. Chen, R.M. Sharp and J.T. Gregory: Mater. Forum, 14 : 130, 1990
- [6] C.S. Lin and M. Meshii: Metall. Trans. B, 25B: 721, 1994
- [7] G.K. Mandal, S.K. Das, R. Balasubramaniam and S.P. Mehrotra: Mater. Sci. Tech., 27: 1265, 2011
- [8] A. Chakraborty and R.K. Ray: Surface & Coatings Tech. 203:1756, 2009
- [9] A. Nishimoto, J. Inagaki and K. Nakaoka: Trans. Iron Steel Inst. Jpn. 26: 807, 1986
- [10] T. Nakamori, Y. Adachi and T. Toki: CAMP-ISIJ, 5: 1637, 1992
- [11] A.R. Marder: Prog. Mat. Sci., 45: 191, 2000
- [12] V. Furdanowicz and C. R. Shastry: Metall. Mater. Trans. A, 30A: 3031, 1999
- [13] E. Baril and G. Lesperance: Metall. Mater. Trans. A, 30A:681, 1999
- [14] C. E. Jordan and A. R. Marder: Metall. Mater. Trans. A, 25A: 937, 1994
- [15] C S LIN, M MESHII and C. C. CHENG, ISIJ Int., 35: 503, 1995
- [16] A.K. Verma, S. Chandra, B.K. Dhindaw and R.D. K. Misra: Mater. Sci. Eng. A, 418 : 335, 2006
- [17] M. Onishi, Y. Wakamatsu and H. Miura: Trans. JIM, 15: 331, 1974
- [18] T. Kanamaru and M. Nakayam: Mater. Sci. Res. Int., 1: 150, 1995
- [19] V.S.S Lopes, M.A. de Faria and P.R. Rios: ISIJ Int., 39: 1204, 1999
- [20] D.R. dos Santos, U.R. Seixas and P.R. Rios: ISIJ Int., 38: 1393, 1998
- [21] T.B. Massalski, Phase Diagrams, ASM Metals Handbook, 3: 206, 1992
- [22] J.H. Hong, S.J. Oh and S.J. Kwon: Intermetallics 11: 207, 2003
- [23] J.M. Long, D.A. Haynes and P.D. Hodgson: Mater. Forum 27 : 62, 2004
- [24] Z.W. Chen, R.M. Sharp and J.T. Gregory: Mater. Sci. Technol. 6: 1173, 1990
- [25] G.K. Mandal, R. Balasubramaniam and S.P. Mehrotra: Metall. Mater. Trans. A, 40A: 637, 2009
- [26] A. Taniyama and M. Arai: Mater. Trans., 45: 2482, 2004
- [27] Syahbuddin, P.R. Munroe, C.S. Laksmi and B. Gleeson: Mater. Sci. Eng. A 251: 87 1998
- [28] U. Chakkingal: Microstructural evolution in galvanized coating during galvannealing, Ph.D. Thesis, Rensselaer Polytechnic Institute, 1994
- [29] Y. Wakamatsu, K. Samura and M. Onishi: J. Jpn. Inst. Met., 41: 664, 1977
- [30] S.R. Teixeira, P.H. Dionisio, E.F. DA Silveira, F.L. Freire, Jr., W.H. Schreiner and I.J.R. Baumvol: Mater. Sci. Eng., 96: 267, 1987